



Integrating 3D printing of polymer matrix composites and metal additive layer manufacturing: surface metallization of 3D printed composite panels through cold spray deposition of aluminium particles

Alessia Serena Perna¹ · Antonio Viscusi¹ · Roberta Della Gatta¹ · Antonello Astarita¹

Received: 9 November 2021 / Accepted: 7 February 2022 / Published online: 28 February 2022
© The Author(s) 2022

Abstract

The integration of metals and polymers in the same component to couple the best properties and advantages of both these classes of materials can be useful for engineering applications. In this scenario, the aim of this paper is to integrate additive manufacturing of composites with cold spray deposition of metal particles: in particular, 3D-printed carbon fibre-reinforced plastics (CFRP) panels were coated with aluminium particles to couple the lightweight and high mechanical properties of CFRP with high wear resistance and hardness of metals. CFRP panels have been produced by using the Fused Filament Fabrication (FFF) technology, then the panels have been coated with aluminium particles by using a low pressure cold spray facility. Panels with various stratification sequences have been produced to investigate the feasibility of the process and to highlight the influence of the lay-up strategy on the whole process; the parameters of the cold spray process have been also optimized to ensure an effective deposition. Adhesion tests, distortion measurements, cross-section observations and surface coverage measurements have been chosen as response outputs to evaluate the effectiveness of the process and to assess the influence of the process parameters. The integration between FFF of CFRPs and cold spray deposition of aluminium particles has been proved, values of surface coverage close to 100% and good values of adhesion strength (close to 4 MPa) have been achieved; moreover, the presence of the fibres, giving a higher stiffness to the substrate, avoids the occurrence of distortion phenomena during the deposition. It was also proved that the printing parameters influence the deposition: an increase in the infill density from 30% to 50% leads to an increase in the adhesion strength up to 40%. In summary, the results obtained proved the feasibility of the process and allowed to enucleate directions of future research.

Keywords Additive manufacturing · Cold spray deposition · Fused filament fabrication · Carbon fibre reinforced plastics · Aluminium alloys

Introduction

The growing demand for engineered materials able to answer the different requests arising during their applications has brought increasing interest toward composite materials, such as the Polymer Matrix Composites (PMCs), whose properties are completely tailorable due to their anisotropic structure [1, 2].

The possibility to obtain high-performance and light-weight structures has attracted a plethora of engineering fields, increasing, in the last few years, the use of PMCs for high-end uses [3]. However, to further expand their fields of application and reduce the issues related to their main drawbacks (such as their poor surface properties and high sensitivity to heat), the metallization of PMCs has been considered as one of the most promising solutions, as studied in the literature [4]. In fact, the surface metallization can enhance the thermal and electrical conductivity of PMCs, improve their erosion behaviour and guarantee lightning protection, which is a crucial aspect to be considered for aircrafts [5, 6].

Among the several techniques allowing to metallize the surface of PMCs, the cold spray (CS) technology emerges,

✉ Antonello Astarita
antonello.astarita@unina.it

¹ Department of Chemical, Materials and Production Engineering, University of Naples, “Federico II”, P.le Tecchio 80, 80125 Naples, Italy

due to the possibility to obtain thick coatings without the risk of damaging the substrate like other metallization techniques [7–9]. CS, in fact, exploits kinetic energy allowing the deposition of micron-sized metallic powders (10–100 μm in diameter [10, 11]) that do not reach the melting temperature during the process, retaining their original properties [12]. The powders are transported by a carrier gas (typically air, nitrogen or helium) that is accelerated at supersonic velocities through a de-Laval nozzle. When the gas/particles stream impacts the surface with a velocity that ranges between 300 and 1200 ms^{-1} , the powders undergo severe plastic deformations and bond together creating a thick, homogeneous coating [13]. The most influencing cold spray process parameters are the gas species, the gas pressure and temperature, and the standoff distance (SoD) [14]. It is known that the deposition process can be effectively carried out if the abovementioned process parameters are properly chosen.

Despite the technological interest in depositing metallic powders on PMCs through cold spray, up to date, there are still numerous knowledge gaps. In fact, it is still not clear what are the best practices to obtain the highest-quality coatings neither the bonding mechanism between the powders and the substrate [15]. As shown in the literature, a trial and error approach is used to find the more suitable CS conditions and different values of the deposition process parameters are used by the researchers for the same powder-substrate combinations [7, 16, 17]. For instance, the authors [18] attained to metallize PEEK polymer substrates by spraying aluminium particles with a gas pressure of 41 bar and by setting the standoff distance at 75 mm. Other authors [19] tried to coat the same substrate typology with Al-based particles by setting the gas pressure in the range 3–5 bar and SoD between 25 and 125 mm. This emphasizes the lack of a single vision in the literature about the best process parameters and equipment to use for an effective deposition. The reason is that the metallization of PMCs through CS is in its early stage and a lot of work needs to be carried out to answer the open questions on this topic.

The last studies proved that, aiming to obtain an effective deposition, the attention must be focused also on the composite lay-up sequence and stratification. The stratification of the substrate must be considered and treated as a process parameter, as well as standoff distance or inlet gas pressure.

Some previous studies of the authors particularly highlight the influence of the matrix layer thickness deposited on the surface of the reinforced polymer, as it affects the deformation of the particles and thus the coating homogeneity [20]. The authors [21] proved that steel 316 L powder can be successfully deposited on a composite substrate with the cold spray technique, suggesting that with a proper choice of the lay-up sequence and matrix layer thickness, along with suitable cold spray process parameters, the deposition

of hard materials can be achievable. For these reasons, it is clear that the composite substrates would need to be tailored to perfectly meet CS requirements, i.e., the customized manufacturing would seem to be a valid route to pursue to obtain high-quality metallic coatings on PMCs.

A plethora of different techniques exists to produce customized substrates. In this scenario, additive manufacturing (AM) techniques appear as the best solutions to obtain tailored composites, by varying the lay-up sequence and stratification, with lower production cost and a high degree of automation, if compared to the traditional ones. Also, the surface morphology can be easily customized through AM due to the possibility of choosing the suitable deposition strategies of both matrix and reinforcements [22].

A well-established technology capable of producing thermoplastic-based composites is the Fused Filament Fabrication [23]. This technology relies on a double mobile nozzle to extrude both matrix and long fibres, which can be printed according to different deposition strategies and printing parameters. Particularly, in this process, polymer filaments are fed into a heated nozzle which allows for the extrusion of polymer strands to build up 3D objects, layer-by-layer, according to Computer-Assisted Design (CAD) 3D models [24]. The adhesion among the extruded polymer strands is the main requirement for fabricating defect-free objects characterised by mechanical properties similar to those typically obtained with conventional extrusion and injection moulding processes [22].

To date, the most used thermoplastic polymers are acrylonitrile butadiene styrene (ABS), polylactic acid (PLA), polycarbonate (PC), polyetheretherketone (PEEK) and nylon due to their relatively low cost as well as their low melting temperatures. Reinforcing materials, such as fibres, can be added to the polymer matrix during printing, in order to produce a composite structure with improved mechanical properties. The reinforcing fibres can be in the form of short or continuous fibres (carbon, fibreglass or kevlar); a dedicated nozzle takes care of depositing a continuous thread of composite fibre on each possible layer [25].

It is clear that FFF technology, as a versatile AM technique, can be integrated successfully with the cold spray technology, for the manufacturing of customized PMC substrates, designed ad hoc to meet the CS requirements. A preliminary study proving the effectiveness of the integrated FFF-CS solution was carried out by Viscusi et al. [26] who evidenced the central role of the surface texturing of the 3D-printed panels (that is possible to regulate through the panel manufacturing route) on the characteristics of the CSed coatings. In particular, the authors proved that the distance among the valleys of the texturing should have a comparable dimension to the feedstock powder diameter with the particles remaining entangled between the traces tracked by two consecutive polymer tracks.

Based on these preliminary results, a more detailed analysis would need to be carried out. For instance, very few works in literature [9, 27–29] deal with the adhesion characteristics of CSed metal coatings on PMCs and, to the authors' best of knowledge, none of these correlated the results from the adhesion tests to both CS process parameters and the printing strategy. Therefore, this research activity aims to study more in-depth the influence of the panels manufacturing strategy on cold spray deposition process for the optimization of the process in its wholeness and characterize the properties of the hybrid 3D-printed-CSed structures obtained.

For this purpose, Onyx-based unreinforced panels, as well as long carbon fibre reinforced panels, were 3D-printed, by adopting different stratification strategies, to point out the influence of the fibre on the deposition. Onyx is a novel nylon-based polymer with short carbon fibres, which was chosen as matrix material for the 3D-printed laminates. Both the sample's typologies (pure Onyx and reinforced panels) were manufactured with three different values of matrix infill density (namely the amount of Onyx used to build a layer) in the core and three different values of matrix layer thickness on the surface. In particular, filler percentages of 30%, 40% and 50% were considered in this activity. Each laminate was metallized through the Low-Pressure Cold Spray technology (LPCS) by setting the same CS process parameters, determined in previous research activities [26, 30, 31]. Micron-sized aluminium powders were used for PMCs metallization. The products were sectioned and then observed through optical, SEM and confocal microscopies. The distortion of each specimen was calculated after the metallization process along with the surface coverage, the particle splat size and distribution; the coating height was also evaluated. The adhesion strength of each coating was measured and correlated with the results from the microscope analyses.

In summary, the influence of the 3D-printed substrate characteristics on CS deposition was analysed by discussing: (i) the effect of the fibres reinforcing the polymer; (ii) the effect of the infill density; (iii) the effect of the superficial layer thickness.

Materials and Methods

3D-Printing of the substrates

The composite laminates were manufactured through FFF technology using a Markforged X7 printer. This printer uses a double nozzle to extrude fibres and matrix filaments. The process was controlled by a built-in laser micrometre that scans the process plate building a map of the surface in order to calibrate the height of the nozzle with a high degree of

precision (1 μm). The materials chosen for the laminates were Onyx for the matrix and long carbon fibres as reinforcement. Onyx is a thermoplastic-based material made of nylon mixed with short carbon fibres. The heat deflection temperature of Onyx is 140 °C. The presence of short fibres guarantees better performances compared to unreinforced nylon. In fact, they modify the behaviour of the nylon on cooling, guaranteeing better dimensional stability by reducing the thermal deformations [31–33].

Long carbon fibres optimized for the printing were chosen as reinforcement: a thin film of nylon encompasses each packet of fibres guaranteeing improved compatibility between matrix and fibres.

The printing process was carried out by setting the temperature of the extrusion nozzle at 260 °C to ensure the melting of the polymer, with a mean speed of 2.39 cm^3/h for the fibres layers and 6.90 cm^3/h for the Onyx layers. Pure Onyx panels as well as reinforced laminates were manufactured in this activity and are referred below as *3D-O* and *3D-F*, respectively.

The infill pattern chosen for the Onyx matrix is triangular in the core and three different percentages filling values (30%, 40% and 50%) were considered for all the samples, as shown in Fig. 1, schematically; meanwhile, the outermost surfaces of the panels were printed with one, two or three layers of 100% fill Onyx filament (the so-called infill solid strategy at 45° [34]) to take the advantages of the resulting higher surface finishing (the details in Fig. 2).

A 0/90 symmetric configuration was set for the reinforced samples which were produced alternating one layer of matrix and one layer of fibres, following the lay-up sequences shown in Fig. 2.

Concerning the matrix layer, firstly the nozzle defines the boundaries of each layer (see Fig. 1) and then the triangular pattern for the matrix core structure.

As summarized in Table 1, 18 different samples were 3D-printed. The table also reports the main geometric characteristics of each specimen. The square-shaped panels (80 × 80 mm) have a thickness in the range 2.0–2.5 mm depending on the number of layers used for the outermost surfaces. Each layer constituting the stratified panel is about 0.125 mm depending on the heated nozzle geometry.

Metallization process through cold spray

Cold spray deposition of micron-sized AlSi10Mg aluminium powders, provided by LPW South Europe, was carried out by means of a Dycomet 423 low-pressure equipment, using air as the carrier gas [13]. The powders used have a mean diameter of 20 μm and have a spherical shape, as previous studies suggested those characteristics as ideal for the deposition [35]. A macrograph and the cumulative size distribution of the chosen powders are portrayed in Fig. 3.

Fig. 1 Illustrative sketch of Onyx-based matrix printing strategy by varying the infill density: (a) 30%, (b) 40%, (c) 50%

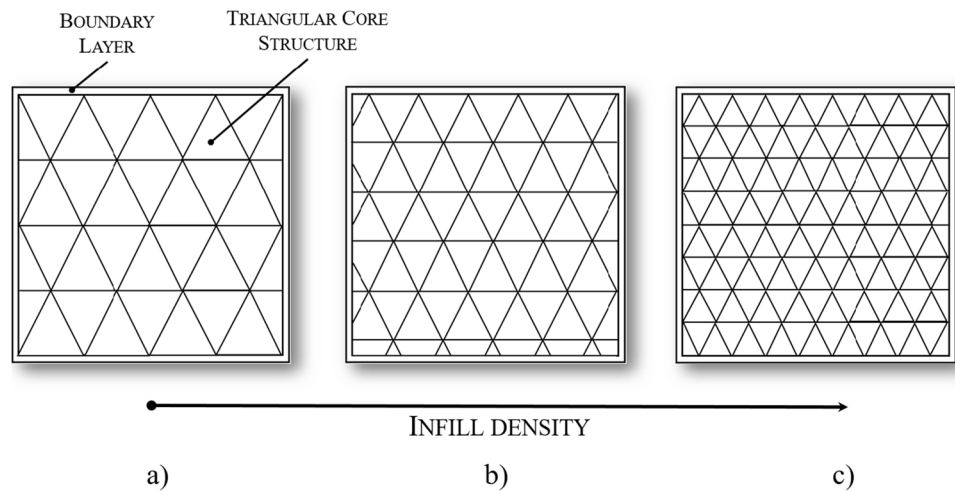
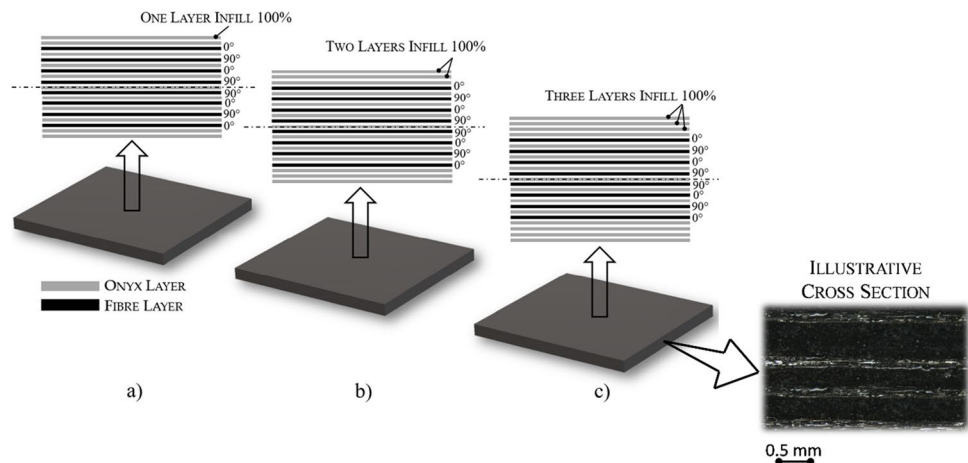


Fig. 2 Simple scheme of a 0/90 symmetric configuration of reinforced samples. The figure highlights the superficial matrix thickness of the outermost surfaces: (a) one layer, (b) two layers; (c) three layers. The insert shows the cross section of the specimen



The spray gun was mounted on a robot (HIGH-Z S-400/T CNC-Technik) to allow for control and repeatability of the coating deposition. To ensure the repeatability of the results three coated tracks were produced on each substrate by setting a single-pass of the spray gun under the same cold spray process conditions. The range of suitable CS process parameters was determined through preliminary experimental tests, which are not here reported for the sake of brevity, as well as literature results [36]. In particular, by setting a travel speed of the spraying gun equal to 1 mm/s for the formation of the track, the inlet gas pressure and temperature were set to 6 bar and 300 °C, respectively, the SoD was set to 45 mm and kept constant during the deposition. It is worth noting that the pressure value was set taking into account that the higher the pressure of the carrier gas, the higher the penetration of particles into the polymer. However, if the pressure of the gas is too high, erosion can take place [37–39]. The gas temperature was chosen considering the glass transition temperature of nylon. As literature studies evidence [40], the deposition should be carried out with a temperature of

the gas impinging on the surface that is higher than the glass transition temperature of the substrate material, in order to guarantee an adequate softening of the impacted surface. Moreover, the gas temperature should be lower than the melting temperature of nylon in order to avoid deterioration phenomena. The stripes observed in Fig. 4 in grey colour represent the single track coatings obtained through the cold spray process. Note that both the pure Onyx and the reinforced specimens with one layer of matrix on the outermost surfaces only are shown, for the sake of brevity.

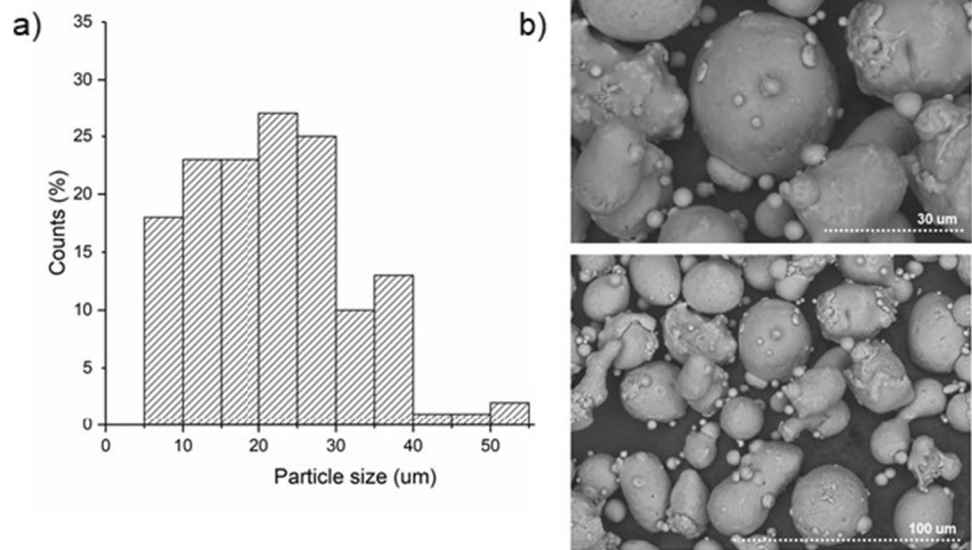
Panels characterization

Confocal acquisitions (LEICA DCM3D Scan) were performed to measure the coating height and analyse the surface morphology of the samples correlating the manufacturing process of the panels with CS deposition mechanisms. A 3D surface taken from a randomized area of the specimen was generated and exported to LeicaMap software in order to analyse the surface topography according to the ISO

Table 1 3D-printed samples manufactured through FFF technology

N. of specimens	ID label	N. of superficial layers	Infill density [%]	Layer thickness [mm]	Panel thickness [mm]	Layup sequence
Pure Onyx panels						
1	3D-O _{1,30}	1	30	0.125	2.0	\\
2	3D-O _{1,40}	1	40	0.125	2.0	\\
3	3D-O _{1,50}	1	50	0.125	2.0	\\
4	3D-O _{2,30}	2	30	0.125	2.25	\\
5	3D-O _{2,40}	2	40	0.125	2.25	\\
6	3D-O _{2,50}	2	50	0.125	2.25	\\
7	3D-O _{3,30}	3	30	0.125	2.5	\\
8	3D-O _{3,40}	3	40	0.125	2.5	\\
9	3D-O _{3,50}	3	50	0.125	2.5	\\
Fibre reinforced panels						
10	3D-F _{1,30}	1	30	0.125	2.0	[0/90]sym
11	3D-F _{1,40}	1	40	0.125	2.0	[0/90]sym
12	3D-F _{1,50}	1	50	0.125	2.0	[0/90]sym
13	3D-F _{2,30}	2	30	0.125	2.25	[0/90]sym
14	3D-F _{2,40}	2	40	0.125	2.25	[0/90]sym
15	3D-F _{2,50}	2	50	0.125	2.25	[0/90]sym
16	3D-F _{3,30}	3	30	0.125	2.5	[0/90]sym
17	3D-F _{3,40}	3	40	0.125	2.5	[0/90]sym
18	3D-F _{3,50}	3	50	0.125	2.5	[0/90]sym

Fig. 3 a Powder size distribution. b SEM micrographs of AISi10Mg aluminium powders

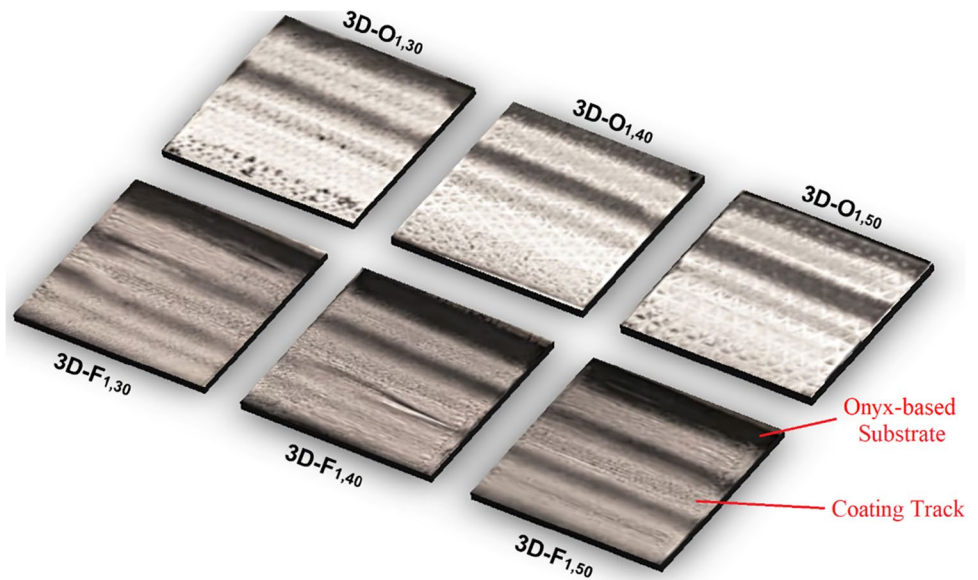


25178-2:2012 standard. The main parameters evaluated were: (i) S_v , (Maximum Valley Depth), namely the depth of the lowest point; (ii) S_p , (Maximum Peak Height), namely the height of the highest point; (iii) S_z that is the maximum height of the surface. It is worth to note that the last parameter was used for the processing and the discussing of the

results obtained; in particular, S_z was considered as a measurement parameter of the coating height, as also shown in literature [20].

The non-reinforced samples showed a visible distortion of the substrate due to the cold spray process, while the reinforced ones showed no distortion at all due to the obvious

Fig. 4 Coating tracks made of AISi10Mg powders produced by CS on both the pure Onyx (3D-O₁) and the reinforced (3D-F₁) specimens with one layer of matrix on the outermost surfaces



stiffening effect of the fibres. To quantify this distortion, indicated as δ (%), and analyse the effects of both the Onyx infill strategy and the surface matrix thickness, the approach of Rokni et al. [19] was followed and the following formula has been used (Eq. 1).

$$\delta = \frac{d - t - d_0}{d_0} \% \quad (1)$$

In Eq. 1, d (μm) is the distance between the lowest and the highest points of the distorted samples calculated as shown in Fig. 5, t (μm) is the coating height and d_0 (μm) is the sample thickness before spraying. Nevertheless, in this work, the distortion was calculated as a percentage of the initial substrate thickness.

The surface of the coated laminates was also analysed through Scanning Electronic Microscope (SEM) Hitachi TM 3000. The SEM images were post-processed by means

of image analyses software (IMAGE J) in order to measure the splat size (namely the size of the powders deformed as a result of the impact on the substrate) and calculate the size distribution of the splat. The latter was evaluated from SEM images by creating a binary mask of the acquired surface and evaluating the pixel threshold. In Fig. 6 the metallic particles are identified in white, while the substrate is evidenced in black. The splats were then divided employing a size filter, working as a virtual sieve, as shown in Fig. 6a and b. Six different diameters ranges were evaluated (considering particles up to 60 μm), for the measurement of the percentual of superficial area occupied by the particles of each size range.

The adhesive strength was measured using following the ASTM D4541 standard and by using a PosiTest ATM. Aluminium dollies with a 10 mm diameter were bonded to the top surface of the cold sprayed deposits using cyanoacrylate glue. Any excess adhesive or coating surrounding the dolly was removed with a drill bit. To assess the success of the

Fig. 5 Cross-section photography of the distorted panel; d is the distance between the lowest and the highest points of the sample

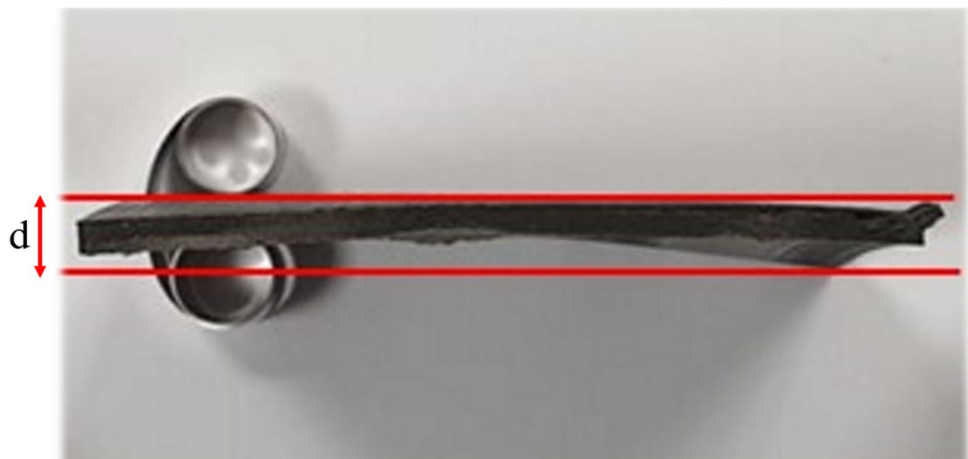
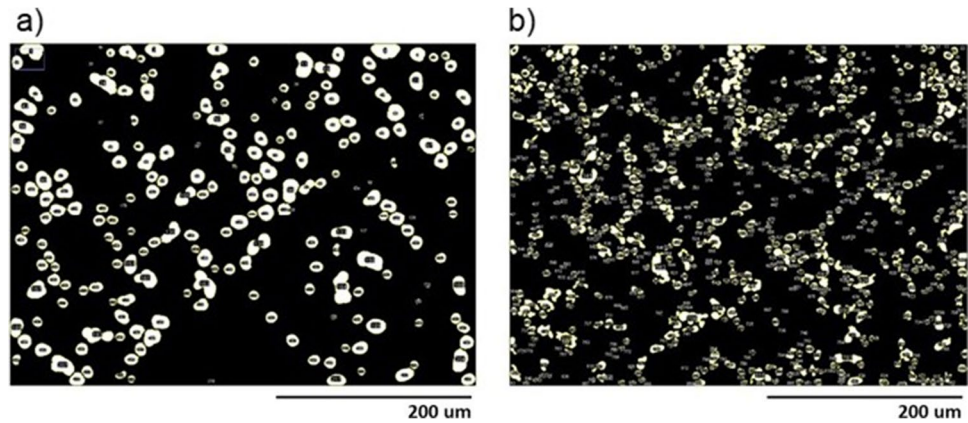


Fig. 6 **a** Particles with a diameter above the mean size of the feedstock powders (20 μm); **b** particles with a diameter below the mean size of the feedstock powders (20 μm)



test, dolly surfaces were analysed by means of an optical microscope in order to quantify the amount of the removed coating.

Results

Confocal analyses: morphology and coating height

As described in the previous paragraphs, one, two or three superficial matrix layers, with a 45 degrees pattern (100% fill Onyx filament), were produced on the outermost surfaces of the panels aiming to analyse the effects of the superficial layer thickness on CS deposition.

It is possible to observe from the confocal microscopies in Fig. 7, which shows the surface morphology of the uncoated pure Onyx samples, that if a single layer of matrix with 45 degrees pattern is printed on the surface, the underlying triangle pattern is well visible. If more layers are printed on the surface, the triangle pattern tends to disappear, as shown in the figure. It is possible to observe the same behaviour for the reinforced panels, not here portrayed for the sake of brevity. This would result in a different behaviour of the particles impacting the target surface, as the particles impinge different surface morphologies, influencing the cold spray deposition. The particles deposition, in fact, would be affected by the layer thickness as

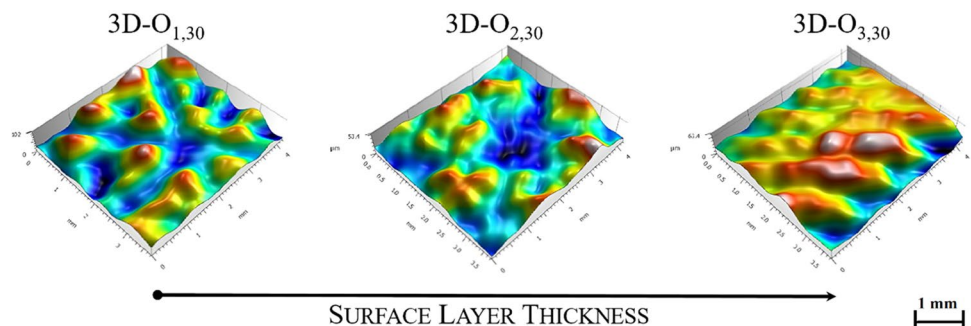
well as the surface pattern. These aspects will be extensively discussed in the following paragraphs.

Confocal analyses were also carried on all the coated samples reported in Table 1. However, for the sake of brevity, the surface morphology of pure Onyx panels with one layer of matrix only on the outermost surfaces, is shown in Fig. 8. From the figure, it is evident the triangular pattern resulted from the manufacturing strategy of the panel. In particular, the coloured blue zones indicate the filling pattern with the Al particles that seem to be entirely impacted within each valley tracked by two consecutive polymer tracks, as also proved in literature [36]. It can be seen that the dimensions of the highlighted triangular structures tend to be smaller with the increase of the infill density (in particular moving from 30% to 50%), with a reduced space between two consecutive valleys.

The height parameters were evaluated from the confocal analyses; the results obtained are reported in Fig. 9.

It can be observed from the figure that the height parameters of the fibre reinforced panels are lower than those of pure Onyx samples, regardless of the infill density and the surface thickness considered. That means the coating height (i.e. S_z) of the 3D-F panels is higher than that of 3D-O samples. These results suggest the higher deformation of the particles impacting the reinforced/stiffer substrates.

Fig. 7 Confocal acquisitions of the top-surface of the uncoated pure Onyx samples



Substrate distortion

Figure 10 shows the pure Onyx panels profiles after the cold spray deposition of Al powder. All the samples exhibit both concave and convex distortion caused by cold sprayed deposits. This substrate distortion was not observed for

carbon reinforced onyx panels and therefore these samples are not considered for this type of analysis. This mismatch between these two types of substrates may be attributed to the lower stiffening of the Onyx panels, which undergo higher thermal deflection upon the deposition.

Fig. 8 Confocal acquisitions of the top surface of the coated pure Onyx samples highlighting the infill density

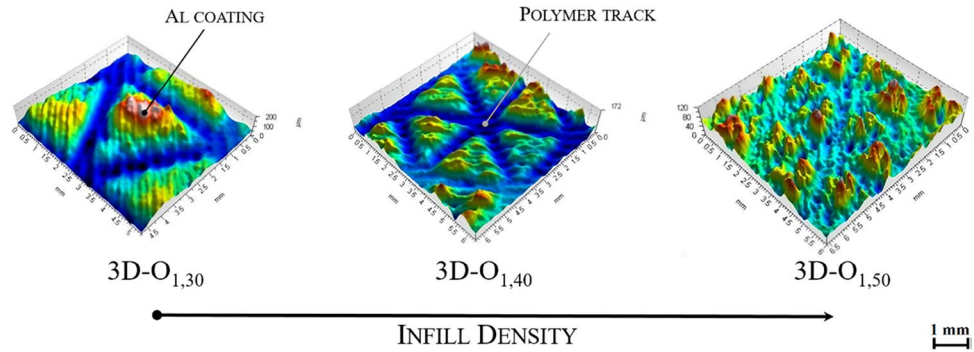


Fig. 9 Height parameters from confocal analyses

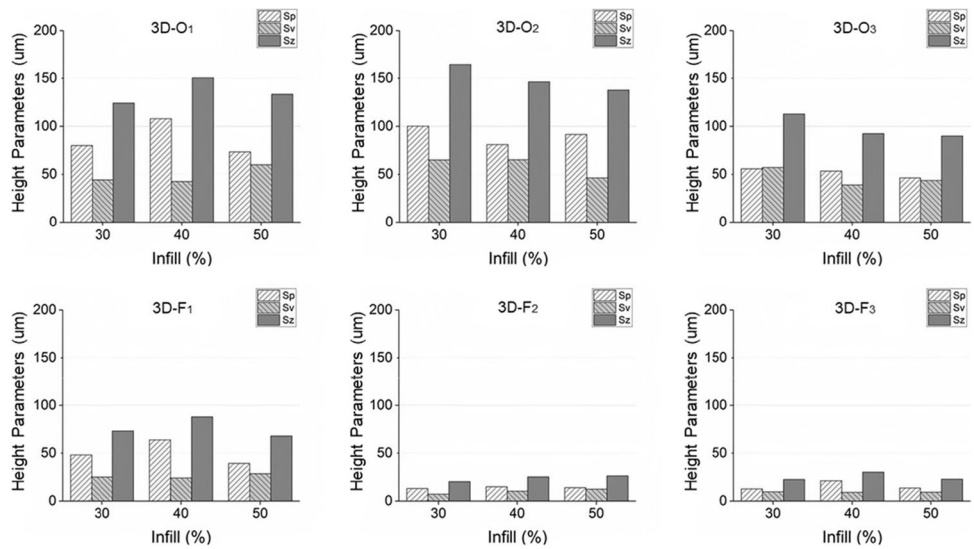
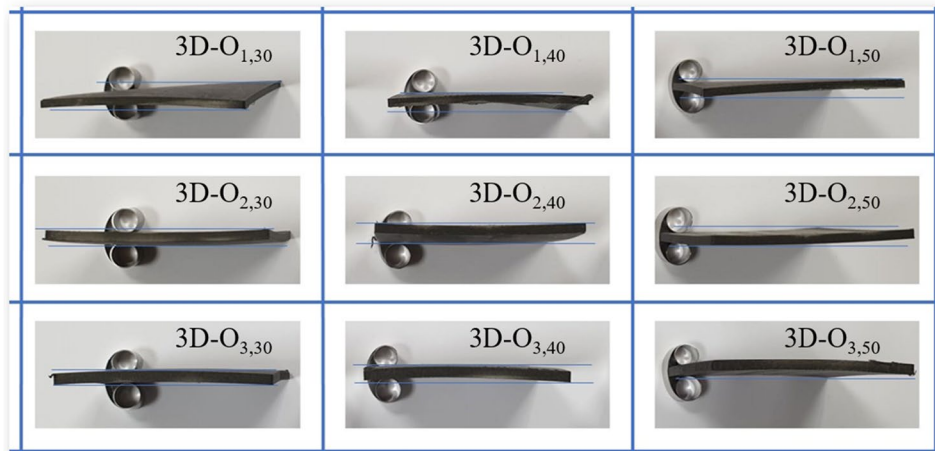


Fig. 10 Pure Onyx panels profiles after the cold spray deposition of AlSi10Mg powder



The results of the substrate distortion calculated through Eq. 1 are reported in Fig. 11. Generally, the results vary with both the matrix infill and the external substrate layers. In detail, as the number of superficial layers increases from one to three, the distortion decreases from a maximum of 225% to a minimum of 65%. At the same time, as the matrix infill increases from 30% to 50%, a decrease in the substrate distortion is observed. Besides, it is evident that the substrate distortion is maximum (up to 225%) in the case of 30% infill and one superficial matrix layer and minimum in the case of 50% infill and three superficial matrix layers. Anyway, it is interesting to note that the effect of the matrix infill percentage tends to flatten when increasing the number of external layers: substrates with one superficial matrix layer showed a wide range of distortion (115–225%) with respect to the different matrix infill, while substrates with three external layers showed a substrate distortion in the same range (60–70%), with no significant dependence on matrix infill. From these results, it is possible to point out that the superficial matrix thickness plays a leading role in the substrate distortion (i.e. substrate stiffening) while the effect of the matrix infill tends to be reduced increasing the number of external layers.

SEM analyses: surface coverage, splat size, splat distribution

The SEM top-view micrographs of the coated surfaces are portrayed in Fig. 12 in order to appreciate the deformation of the particles and analyse the effects of the fibres reinforcing the polymer, the infill density and the superficial layer thickness on the surface coverage of the samples.

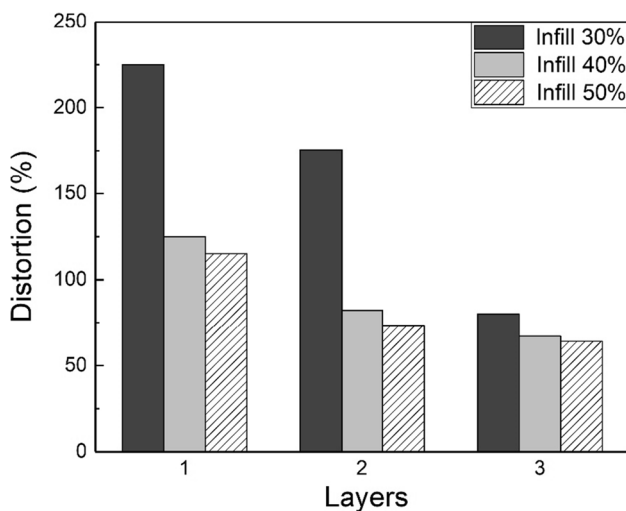


Fig. 11 Results of the substrate distortion of pure Onyx panels calculated through Eq. 1

It can be observed an overall good coverage for all the specimens analysed, characterised by the presence of few voids among the particles. The coatings obtained on fibre reinforced specimens appear more homogeneous due to the increased deformation of the particles, caused by the stiffening effect of the fibres. This can be furtherly highlighted by analysing the particles splat size results, as shown in Fig. 13.

It can be noticed that the mean splat size is slightly higher for the fibre reinforced panels due to the higher stiffness of the reinforced panels that promote the deformation of the particles. This is also confirmed by the splat size distribution analysis. As an example, Fig. 14 shows a comparison between 3D-O_{2,30} and 3D-F_{2,30} panels: it is possible to observe that the size distribution is more homogeneous for the fibre reinforced panels as more particles are deformed and a higher percentage of bigger particles is present and cover the substrate surface.

Adhesion Strength

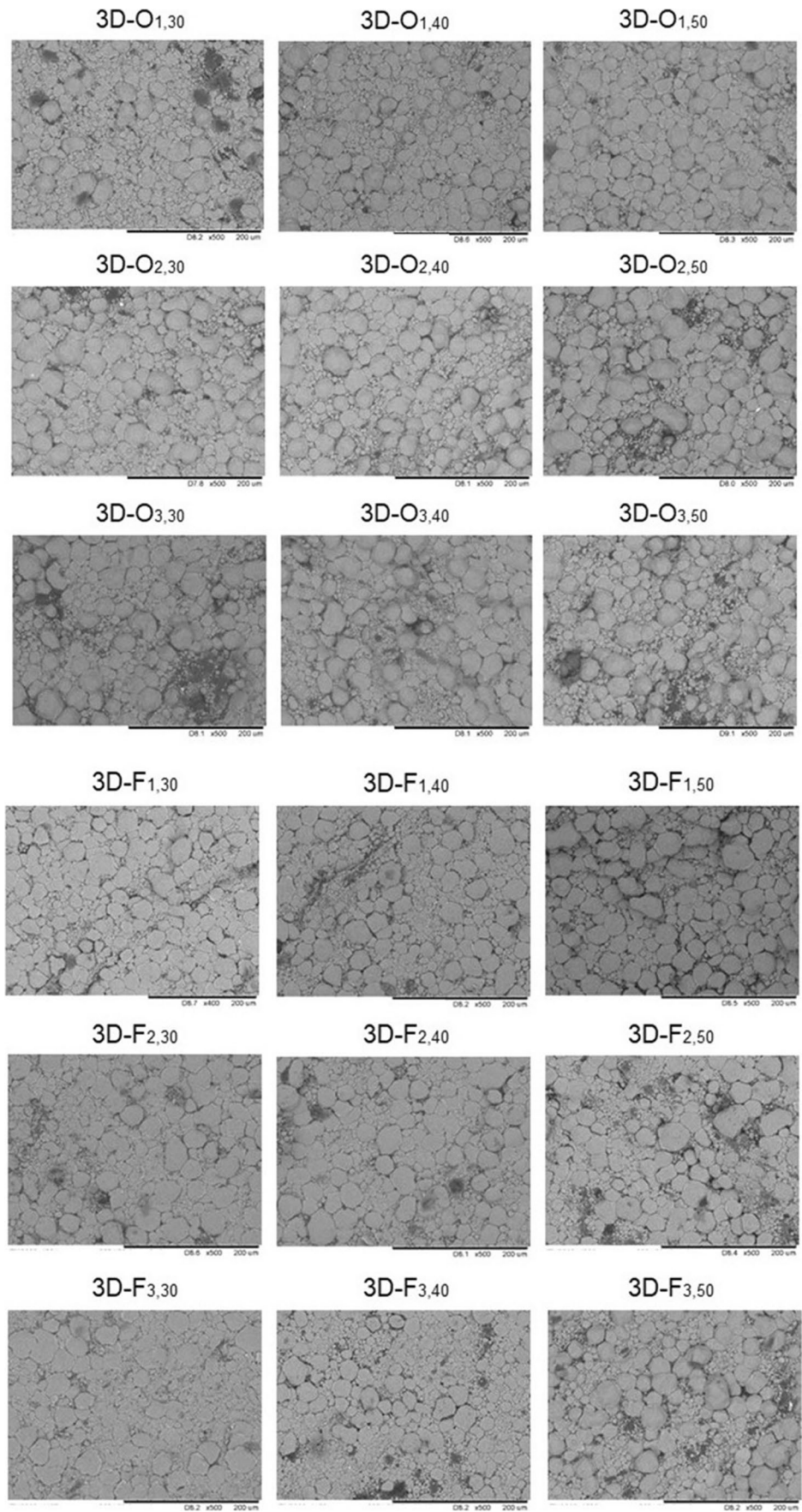
The results of the adhesion strength tests are shown in Fig. 15. By observing these figures, the cold sprayed coatings on pure Onyx samples show a greater adhesion strength (up to 5.8 MPa) compared to the ones on carbon reinforced Onyx (up to 4.2 MPa). These values are in the same range reported previously for metallic coatings/polymeric substrates [16].

As seen in Fig. 15a, for coatings on pure Onyx panels, the adhesion strength varies from a minimum of 3 MPa to a maximum of 5.8 MPa. When increasing the matrix infill at a fixed number of superficial layers, the coating adhesion increases. However, as also observed for the substrate distortion, the scatter among the three panels (30%, 40% and 50%), in terms of adhesion strength values, tends to be reduced when increasing the number of the superficial matrix layers.

On the other hand, as seen in Fig. 15b, in the case of carbon reinforced onyx substrates, the variation of the adhesion strength is less pronounced and results in the range from 2.6 to 4.2 MPa. Also in this case, at a fixed number of superficial layers, the adhesion generally increases when increasing the matrix infill.

To assess the effectiveness of the adhesion tests, residual coating particles adhered on the dolly surface have been investigated through optical analysis. In particular, three different morphologies of the fracture surface were found: (1) AlSi10Mg coating, (2) Onyx substrate and (3) glue or other impurities. The measure of the area fractions of the dolly that are interested by the coating, or the substrate or other impurities were calculated by SEM images. For the sake of brevity, only the results obtained for pure Onyx samples are reported in Fig. 16.

Fig. 12 SEM top-view micrographs of the coated surfaces



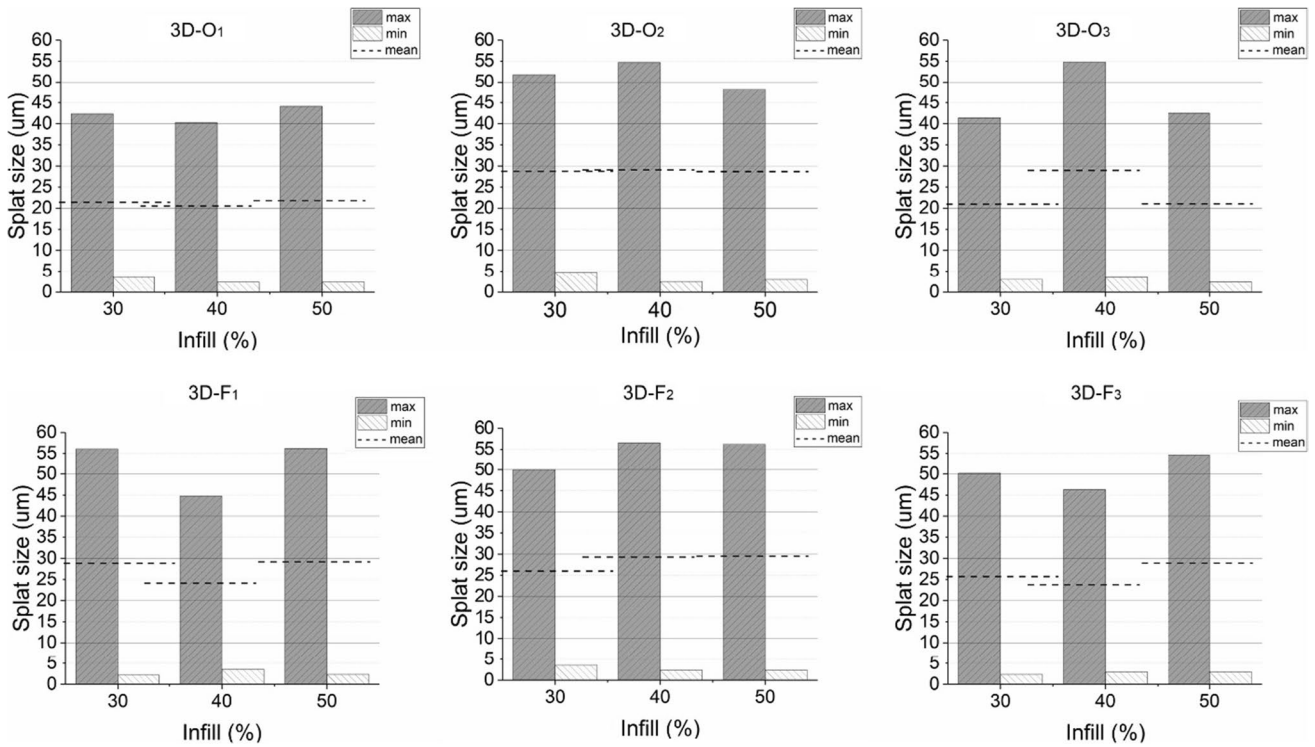


Fig. 13 Particles splat size from SEM images. The dotted lines evidence the mean splat size

Fig. 14 Splat size distribution analysis for 3D-O_{2,30} e 3D-F_{2,30} samples

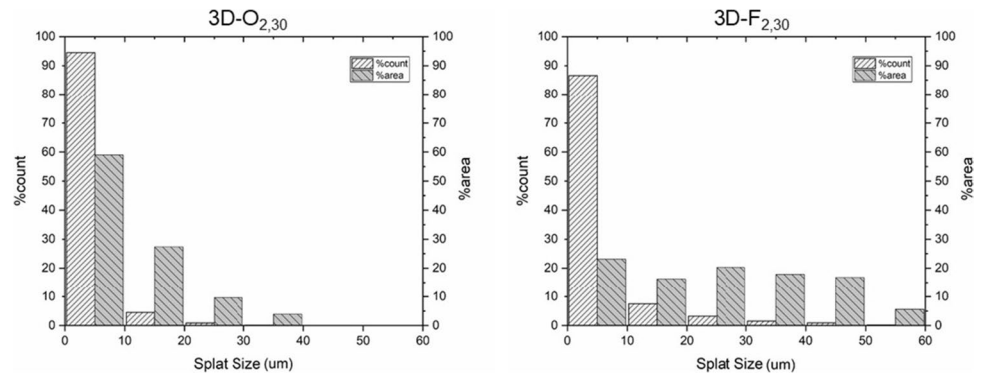
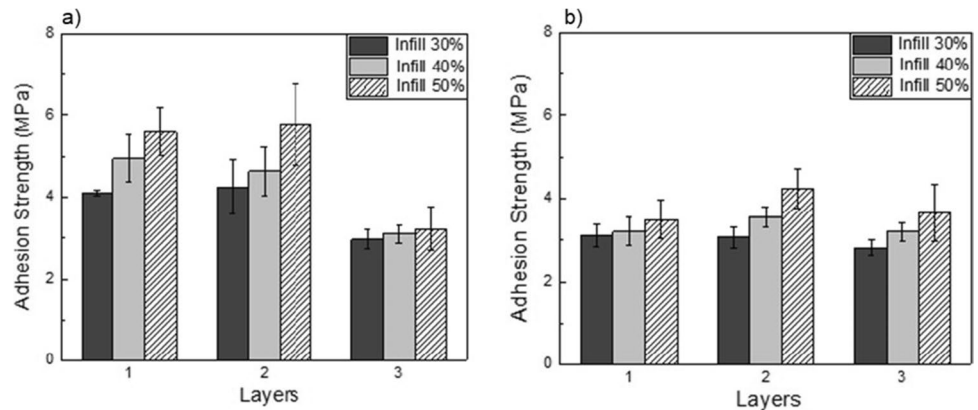


Fig. 15 Results of the adhesion strength tests for both pure Onyx (a) and reinforced (b) samples



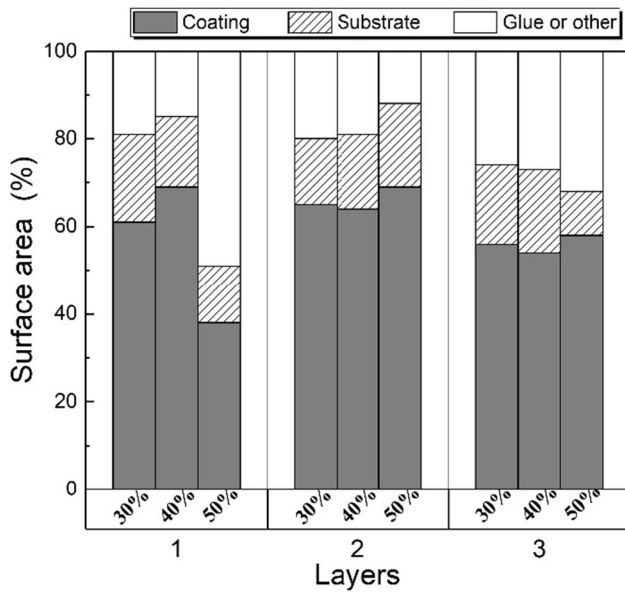


Fig. 16 Area fractions of the dolly surface for the pure Onyx samples

The results presented in Fig. 16 prove that the surfaces of the dollies after the test are covered for over 60% by Al coating. These results suggest that the bonding between Onyx substrate and Al coating is weaker than the bonding between the glue and the coating, thus the test was properly carried out.

Discussion

As pointed out in previous works [36], the manufacturing strategy of the substrate can have a great influence on the cold spray deposition process. For this reason, in order to highlight the influence of the substrate characteristics on cold spray deposition, the following features were considered and below discussed: (i) the effect of the fibres

reinforcing the polymer panels, (ii) the effect of the infill density, (iii) the effect of the superficial layer thickness.

Effect of fibres

The results portrayed in the previous paragraphs have been processed in order to highlight and discuss the influence of fibres reinforcing the Onyx panels on the cold spray deposition process, as shown in Fig. 17.

Figure 17a illustrates the comparison, in terms of mean coating height, between the pure Onyx and reinforced panels. As shown in the figure, the reinforced panels globally have a value of the coating height that is lower of about 70% compared to the unreinforced panels. The lowering of the coating height is usually due to two main phenomena occurring during the deposition: (i) the deformation of the particles, (ii) the penetration of the particles into the substrate [41].

Figure 17b portrays the percentage of particle splats having a diameter higher than the mean diameter of the feed-stock particles, so it represents the percentage of particles that experience deformation upon impact with the substrate. Looking at Fig. 17b, it is possible to notice that 60% of the particles sprayed on the reinforced substrate have undergone a severe deformation, while only 50% of the particles sprayed on the unreinforced substrates have reached a diameter higher than the mean diameter of the processing powders. Consequently, it is possible to assert that the coating produced on the reinforced panels is more deformed. As proved in literature [20], this is due to the stiffening effect of the reinforcement.

Moreover, it is possible to observe from the cross-section micrographs of the specimens in Fig. 18 (where 3D-F_{3,40} and 3D-O_{3,40} panels are considered as examples) that the coatings produced on the reinforced panels have a lower penetration depth (about 13 μm) compared to

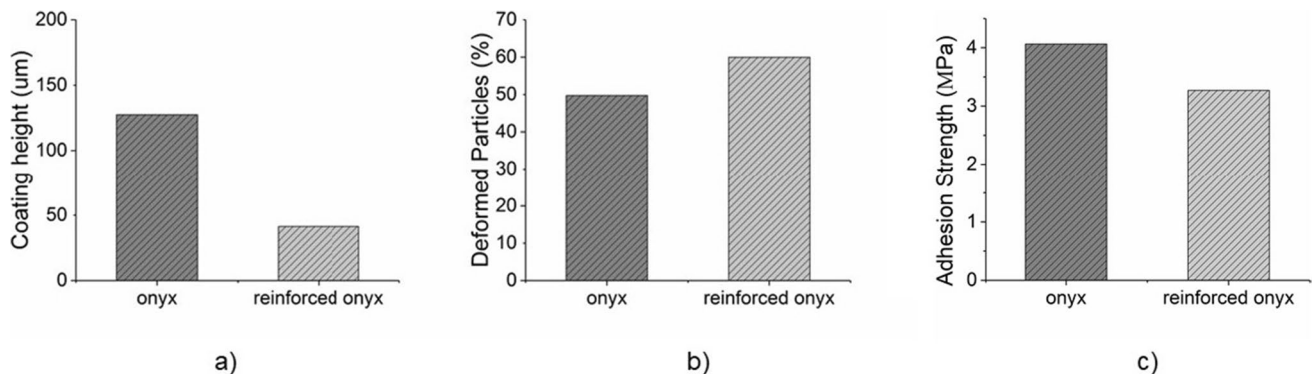
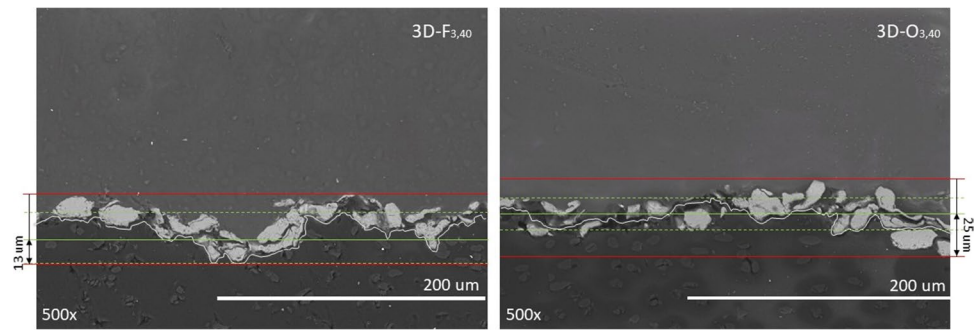


Fig. 17 Effect of the fibres on cold spray deposition. **a** Mean coating height of pure Onyx and fibre reinforced panels; **b** percentage of deformed particles due to deposition; **c** adhesion strength values

Fig. 18 SEM images of 3D-F_{3,40} and 3D-O_{3,40} samples. The penetration depth is calculated as the distance of the deepest point reached by the coating from the substrate main plane



the coatings obtained on the unreinforced panels (about 25 μm), due to constraining effect of the fibres.

This suggests that the prevailing phenomenon causing the lowering of the coating height on the reinforced panels is the plastic deformation of the particles caused by the stiffening effect of the fibres.

By looking at the results illustrated in Fig. 17c, it is possible to notice that the coating produced on the reinforced panels results less adhered with the substrate, compared to the coating produced on the unreinforced panels. This result highlights that the higher deformation of the coating produced on the reinforced panels does not determine a higher adhesion, contrary to what was observed for metallic coatings on metallic substrates [42, 43]. For this reason, in order to obtain a higher adhesion, it would be necessary to promote a greater penetration of the particles into the substrates, while the deformation of the particles seems to be not so important for adhesion.

In conclusion, it is possible to assert that the presence of the fibres leads to more homogeneous coatings (as shown in SEM micrographs in Fig. 12), but causes an overall worsening of the adhesion of the coating on the substrate.

Effect of the infill density

The influence of the infill density on the mechanisms ruling the adhesion of the metallic particles on the 3D-printed substrates is evidenced in the graphs in Fig. 19.

From Fig. 19a it is possible to notice an overall lowering of the coating height when the infill percentage is increased moving from 30% to 50%. The lowering of the coating height can be ascribed to a higher deformation of the particles, as confirmed by Fig. 19b, where it is possible to notice that for an infill density of 30%, about 37% of the particles are deformed acquiring a diameter higher than the mean diameter of the feedstock particles, while for an infill density of the 50%, about the 65% of the particles are highly deformed. The higher deformation of the particles would seem to be determined by the stiffening of the panels when the infill density is increased. This is confirmed by the results obtained by measuring the substrate distortion presented in the previous paragraphs. In fact, the panels having an infill density of 30%, portray higher values of distortion than the panels that have infill densities of 40% and 50%, regardless of the number of onyx layers on the surface, evidencing an increasing stiffness of the panels when the infill density is increased. On the basis of the results obtained in the previous paragraph, it would be reasonable

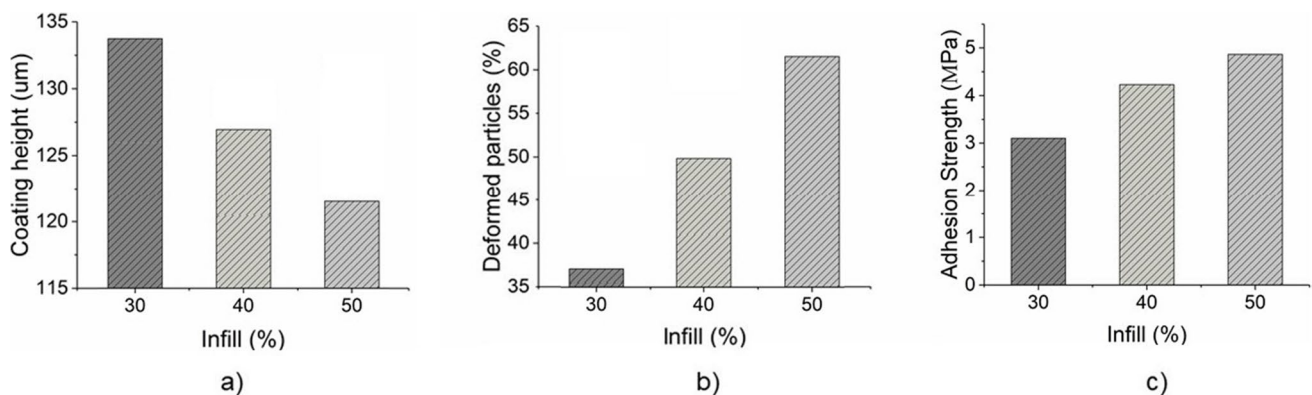


Fig. 19 Influence of the infill density on CS deposition. **a** Mean coating height; **b** percentage of deformed particles; **c** adhesion strength values

to expect that a better adhesion is obtained on the less stiff panels with the particles that should penetrate profoundly the substrate; however, looking at Fig. 19c it is possible to notice that increasing the infill density, the adhesion values increase as well. In fact, the stiffening effect caused by the increase of the infill density is not as relevant as the stiffening effect caused by the fibres, as proved by the fact the reinforced panels do not experience important distortion during the deposition process. The reason is that there is a further phenomenon that prevails over the stiffening effect in determining the adhesion values. As suggested by previous literature studies [36], the superficial texturing can have a remarkable influence on the adhesion mechanisms [44, 45]. Starting from a value of the infill density equal to 30% and moving toward 50%, there is a densification of the texturing (see Fig. 8 above reported) that causes the entanglement of the particles between two consecutive polymer tracks.

For these reasons, the adhesion of the coating was proved to be stronger for the denser panels, as it is more difficult to remove the entangled particles from the substrate. The main result of this study is that by lowering the distance between the polymer tracks (namely increasing the infill density) it is possible to increase the adhesion between the metallic particles and the polymeric substrate: increasing the infill density from 30% to 50%, the adhesion strength increases up to 40%.

Effect of the superficial matrix layer thickness

It is possible to observe the influence of the superficial matrix layer thickness on the cold spray deposition process of metals-to-polymers, by looking at the results presented in Fig. 20.

Looking at Fig. 20a, it is possible to notice a decrease of the coating height when two layers of Onyx are deposited on the top surface of the panel; the same trend was observed when a further layer of matrix on the surface of

the panel is added. This phenomenon is due to the deformation of the particles that tend to deform greatly with the increase of the number of the superficial layers, as shown in Fig. 20b. In fact, it is possible to observe that the percentage of deformed particles is about 45% for the panel with a single layer on the surface while, when two layers are deposited, 52% of the particles are deformed. Adding a third Onyx layer, the coating appears much more deformed as almost 55% of the splats have a higher diameter than the mean diameter of the processing powders. This behaviour is coherent with the trend of the coating height. The reason is that the particles impact on a more rigid surface, as proved by the results above presented. In particular, it was found in the previous paragraphs that the superficial matrix thickness plays a leading role in the substrate distortion, i.e. in the substrate stiffening, as the panels with three external layers showed a reduced substrate distortion (see Fig. 11). As for adhesion strength values, by looking Fig. 20c, it can be seen that by adding two layers on the top surface of the panel, the adhesion reduces compared to the case when a single layer is deposited on the surface. Moreover, by adding a further layer on the surface, a further worsening of the adhesion behaviour can be observed. The reasons are to be found in the stiffness of the panels that tend to increase with the number of superficial layers. In fact, the particles that impact on a softer substrate (like the panels with a single layer of matrix on the surface) can penetrate greatly the polymer surface anchoring with the surrounding polymeric material [46] so resulting in higher values of adhesion strength.

In summary, increasing the superficial matrix layer thickness it is possible to produce more homogenous metallic coatings (made by more deformed particles) but characterised by a lower adhesion with the polymeric substrate: increasing the number of superficial layers from 1 to 3, the adhesion strength reduces up to 25%.

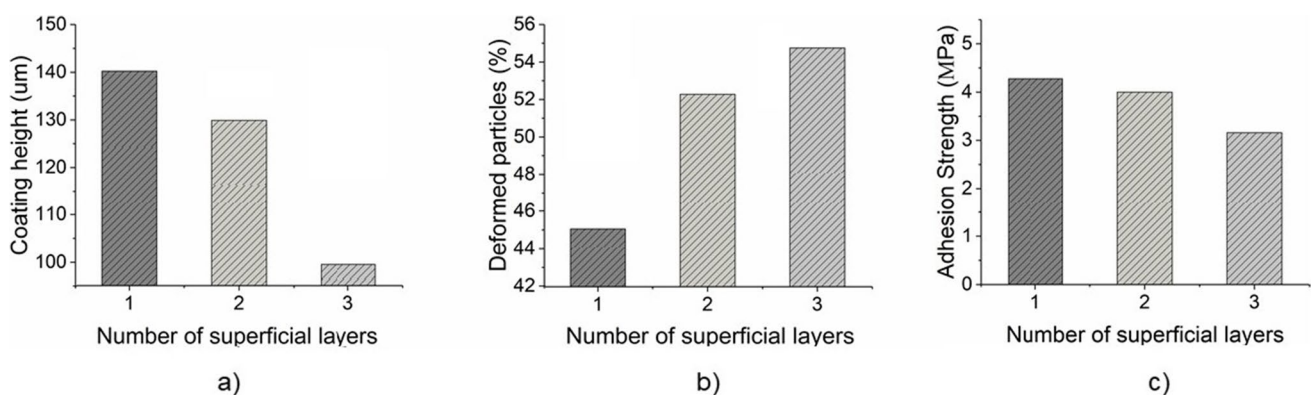


Fig. 20 Influence of the superficial matrix layer thickness. **a** Mean coating height; **b** percentage of deformed particles; **c** adhesion strength values

Conclusions

The cold spray deposition of Al particles on 3D-printed panels was studied by focusing attention on the influence of the manufacturing strategy of PMCs on the metallization process. In particular, in this research activity, the effect of the fibres reinforcing the polymer, the effect of the infill density and the influence of the superficial layer thickness were analysed in detail. Based on the above discussed experimental results, the following conclusions can be drawn:

- The integration between FFF of CFRP and cold spray deposition of aluminium particles has been proved, values of surface coverage close to 100% and good values of adhesion strength (close to 4 MPa) have been achieved when the processing conditions are properly set;
- It has been proved that the lay-up sequence of the composite substrate has a fundamental role in the production of these hybrid structures, the lay-up sequence is more important than the deposition conditions;
- The presence of the fibres leads to more homogeneous coatings (as shown in SEM micrographs in Fig. 12) but causes an overall worsening of the adhesion of the coating on the substrate.
- Increasing the infill density leads to an increase of the adhesion strength between the metallic particles and the polymeric substrate: increasing the infill density from 30% to 50%, the adhesion strength increases up to 40%.
- Increasing the superficial matrix layer thickness, it is possible to produce more homogenous metallic coatings (made by more deformed particles) but characterised by a lower adhesion with the polymeric substrate: increasing the number of superficial layers from 1 to 3, the adhesion strength reduces up to 25%.
- The presence of the fibres, giving a higher stiffness to the substrate, avoids the occurrence of distortion phenomena during the deposition;
- The growth of the coating is still an issue, the maximum thickness achievable is lower than 100 μm .

Moving from these conclusions some recommendations of future work can be suggested:

- The adhesion between the powders and the substrate must be improved, a higher adhesion strength will widen the field of application of these structures;
- The growth of the coating must be also studied, to date, it is possible to obtain a coating with a limited thickness;
- The deposition on thermoset polymers should also be investigated;
- Once the adhesion strength is improved and the growth of the coating has been obtained, the printing of com-

plex shaped metal features on composite panels should be investigated.

Acknowledgements The authors want to thank the Italian Ministry for University and Research (MUR) for funding the whole research activity through the grant: PRIN 2017 – COSMEC.

Declarations

Conflict of Interest The authors declare that they have no conflict of interest.

Open Access This article is licensed under a Creative Commons Attribution 4.0 International License, which permits use, sharing, adaptation, distribution and reproduction in any medium or format, as long as you give appropriate credit to the original author(s) and the source, provide a link to the Creative Commons licence, and indicate if changes were made. The images or other third party material in this article are included in the article's Creative Commons licence, unless indicated otherwise in a credit line to the material. If material is not included in the article's Creative Commons licence and your intended use is not permitted by statutory regulation or exceeds the permitted use, you will need to obtain permission directly from the copyright holder. To view a copy of this licence, visit <http://creativecommons.org/licenses/by/4.0/>.

References

1. Rajak DK, Pagar DD, Kumar R, Pruncu CI (2019) Recent progress of reinforcement materials: a comprehensive overview of composite materials. *J Mater Res Technol* 8:6354–6374. <https://doi.org/10.1016/j.jmrt.2019.09.068>
2. Yao SS, Jin FL, Rhee KY et al (2018) Recent advances in carbon-fiber-reinforced thermoplastic composites: a review. *Compos Part B Eng* 142:241–250. <https://doi.org/10.1016/j.compositesb.2017.12.007>
3. Sajan S, Philip Selvaraj D (2021) A review on polymer matrix composite materials and their applications. *Mater Today Proc*, 47:5493–5498. <https://doi.org/10.1016/j.matpr.2021.08.034>
4. Parmar H, Tucci F, Carlone P, Sudarshan TS (2021) Metallization of polymers and polymer matrix composites by cold spray: state of the art and research perspectives. *Int Mater Rev*. <https://doi.org/10.1080/09506608.2021.1954805>
5. Lan M, Cai J, Zhang D et al (2014) Electromagnetic shielding effectiveness and mechanical property of polymer-matrix composites containing metallized conductive porous flake-shaped diatomite. *Compos Part B Eng* 67:132–137. <https://doi.org/10.1016/j.compositesb.2014.06.029>
6. Małachowska A, Pawłowski L, Winnicki M et al (2015) The possibility of cold spray process application to obtain electrically conductive coatings on polymers. *Proc Int Therm Spray Conf 2*:1159–1164. <https://doi.org/10.13140/RG.2.1.3267.9848>
7. Che H, Gagné M, Rajesh PSM et al (2018) Metallization of carbon fiber reinforced polymers for lightning strike protection. *J Mater Eng Perform* 27:5205–5211. <https://doi.org/10.1007/s11665-018-3609-y>
8. Huang G, Wang H, Li X et al (2018) Deposition efficiency of low pressure cold sprayed aluminum coating. *Mater Manuf Process*. <https://doi.org/10.1080/10426914.2017.1415443>
9. Perna AS, Astarita A, Carlone P et al (2021) Characterization of cold-spray coatings on fiber-reinforced polymers through

- nanoindentation tests. *Metals (Basel)* 11:1–16. <https://doi.org/10.3390/met11020331>
10. King PC, Jahedi M (2010) Relationship between particle size and deformation in the cold spray process. *Appl Surf Sci* 256:1735–1738. <https://doi.org/10.1016/j.apsusc.2009.09.104>
 11. Raelison RN, Xie Y, Sapanathan T et al (2018) Cold gas dynamic spray technology: a comprehensive review of processing conditions for various technological developments till to date. *Addit Manuf* 19:134–159. <https://doi.org/10.1016/j.addma.2017.07.00>
 12. Champagne V, Helfritsch D (2016) The unique abilities of cold spray deposition. *Int Mater Rev* 61:437–455. <https://doi.org/10.1080/09506608.2016.1194948>
 13. Stoltenhoff T, Kreye H, Richter HJ (2002) An analysis of the cold spray process and its coatings. *J Therm Spray Technol* 11:542–550. <https://doi.org/10.1361/105996302770348682>
 14. Arabgol Z, Villa Vidaller M, Assadi H et al (2017) Influence of thermal properties and temperature of substrate on the quality of cold-sprayed deposits. *Acta Mater* 127:287–301. <https://doi.org/10.1016/j.actamat.2017.01.040>
 15. Hussain T, McCartney DG, Shipway PH, Zhang D (2009) Bonding mechanisms in cold spraying: the contributions of metallurgical and mechanical components. *J Therm Spray Technol* 18:364–379. <https://doi.org/10.1007/s11666-009-9298-1>
 16. Ganesan A, Yamada M, Fukumoto M (2013) Cold spray coating deposition mechanism on the thermoplastic and thermosetting polymer substrates. In: *Journal of thermal spray technology*. pp 1275–1282 <https://doi.org/10.1007/s11666-013-9984->
 17. Lupoi R, O'Neill W (2010) Deposition of metallic coatings on polymer surfaces using cold spray. *Surf Coatings Technol* 205:2167–2173. <https://doi.org/10.1016/j.surfcoat.2010.08.128>
 18. Feng P, Rokni MR, Nutt SR (2021) Depositing aluminum onto PEKK composites by cold spray. *J Therm Spray Technol* 30:385–393. <https://doi.org/10.1007/s11666-020-01125-3>
 19. Rokni MR, Feng P, Widener CA, Nutt SR (2019) Depositing Al-Based metallic coatings onto polymer substrates by cold spray. *J Therm Spray Technol* 28:1699–1708. <https://doi.org/10.1007/s11666-019-00911-y>
 20. Della Gatta R, Viscusi A, Perna AS et al (2021) Cold spray process for the production of AlSi10Mg coatings on glass fibers reinforced polymers. *Mater Manuf Process* 36:106–121. <https://doi.org/10.1080/10426914.2020.1813895>
 21. Della Gatta R, Viscusi A, Perna AS et al (2021) Feasibility of steel powder deposition on composites through cold spray. *Mater Manuf Process* 36:281–291. <https://doi.org/10.1080/10426914.2020.1832693>
 22. Brenken B, Barocio E, Favaloro A et al (2018) Fused filament fabrication of fiber-reinforced polymers: a review. *Addit Manuf* 21:1–16. <https://doi.org/10.1016/j.addma.2018.01.002>
 23. Kandananond K (2020) Optimization of fused filament fabrication system by response surface method. *Int J Metrol Qual Eng* 11: <https://doi.org/10.1051/ijmqe/2020002>
 24. García Plaza E, Núñez López PJ, Caminero Torija MÁ, Chacón Muñoz JM (2019) Analysis of PLA geometric properties processed by FFF additive manufacturing: effects of process parameters and plate-extruder precision motion. *Polymers (Basel)* 11:<https://doi.org/10.3390/polym11101581>
 25. Jiang D, Smith DE (2017) Anisotropic mechanical properties of oriented carbon fiber filled polymer composites produced with fused filament fabrication. *Addit Manuf* 18:84–94. <https://doi.org/10.1016/j.addma.2017.08.006>
 26. Viscusi A, Astarita A, Borrelli D, et al (2021) On the influence of manufacturing strategy of 3D-Printed polymer substrates on cold spray deposition. *Esaform* 2021. <https://doi.org/10.25518/esaform21.3003>
 27. Bortolussi V, Figliuzzi B, Willot F et al (2020) Electrical conductivity of metal–polymer cold spray composite coatings onto carbon fiber-reinforced polymer. *J Therm Spray Technol* 29:642–656. <https://doi.org/10.1007/s11666-020-00999-7>
 28. Che H, Chu X, Vo P, Yue S (2017) Cold spray of mixed metal powders on carbon fibre reinforced polymers. *Surf Coatings Technol* 329:232–243. <https://doi.org/10.1016/j.surfcoat.2017.09.052>
 29. Lomonaco P, Weiller S, Feki I, et al (2019) Cold spray technology to promote conductivity of short carbon fiber reinforced polyether-ether-ketone (PEEK). In: *Key engineering materials*. pp 459–464 <https://doi.org/10.4028/www.scientific.net>
 30. Della Gatta R, Astarita A, Borrelli D, et al (2021) Manufacturing of aluminum coating on 3D-Printed Onyx with cold spray technology. *Esaform* 2021. <https://doi.org/10.25518/esaform21.858>
 31. Perna AS, Astarita A, Borrelli D, et al (2021) Fused filament fabrication of ONYX-Based composites coated with aluminum powders: a preliminary analysis on feasibility and characterization. *Esaform* 2021. <https://doi.org/10.25518/esaform21.4017>
 32. Bárník F, Vaško M, Handrik M et al (2019) Comparing mechanical properties of composites structures on Onyx base with different density and shape of fill. *Transp Res Procedia* 40:616–622. <https://doi.org/10.1016/j.trpro.2019.07.088>
 33. Ramalingam PS, Mayandi K, Balasubramanian V et al (2020) Effect of 3D printing process parameters on the impact strength of onyx – glass fiber reinforced composites. *Mater Today Proc* 45:6154–6159. <https://doi.org/10.1016/j.matpr.2020.10.467>
 34. Sanei SHR, Popescu D (2020) 3d-printed carbon fiber reinforced polymer composites: a systematic review. *J Compos Sci* 4: <https://doi.org/10.3390/jcs4030098>
 35. Ganesan A, Affi J, Yamada M, Fukumoto M (2012) Bonding behavior studies of cold sprayed copper coating on the PVC polymer substrate. *Surf Coatings Technol* 207:262–269. <https://doi.org/10.1016/j.surfcoat.2012.06.086>
 36. Viscusi A, Della Gatta R, Delloro F et al (2021) A novel manufacturing route for integrated 3D-printed composites and cold-sprayed metallic layer. *Mater Manuf Process*. <https://doi.org/10.1080/10426914.2021.1942908>
 37. Gillet V, Aubignat E, Costil S et al (2019) Development of low pressure cold sprayed copper coatings on carbon fiber reinforced polymer (CFRP). *Surf Coatings Technol* 364:306–316. <https://doi.org/10.1016/j.surfcoat.2019.01.011>
 38. Moridi A, Hassani-Gangaraj SM, Guagliano M (2013) A hybrid approach to determine critical and erosion velocities in the cold spray process. *Appl Surf Sci* 273:617–624. <https://doi.org/10.1016/j.apsusc.2013.02.089>
 39. Yin S, Liao HL, Wang XF (2014) Euler based finite element analysis on high velocity impact behaviour in cold spraying. *Surf Eng* 30:309–315. <https://doi.org/10.1179/1743294413Y.0000000240>
 40. Che H, Vo P, Yue S (2019) Investigation of cold spray on polymers by single particle impact experiments. *J Therm Spray Technol* 28:135–143. <https://doi.org/10.1007/s11666-018-0801-4>
 41. Giraud D, Borit F, Guipont V, et al (2012) Metallization of a polymer using cold spray: application to aluminum coating of polyamide 66. In: *Proceedings of the international thermal spray conference*. pp 265–270
 42. Moridi A, Hassani-Gangaraj SM, Guagliano M, Dao M (2014) Cold spray coating: review of material systems and future perspectives. *Surf Eng* 30:369–395. <https://doi.org/10.1179/1743294414Y.0000000270>
 43. Schmidt T, Gärtner F, Assadi H, Kreye H (2006) Development of a generalized parameter window for cold spray deposition. *Acta Mater* 54:729–742. <https://doi.org/10.1016/j.actamat.2005.10.005>
 44. Kromer R, Danlos Y, Aubignat E et al (2017) Coating deposition and adhesion enhancements by laser surface texturing—metallic particles on different classes of substrates in cold spraying

- process. *Mater Manuf Process* 32:1642–1652. <https://doi.org/10.1080/10426914.2017.1364750>
45. Viscusi A, Astarita A, Della GR, Rubino F (2019) A perspective review on the bonding mechanisms in cold gas dynamic spray. *Surf Eng* 35:743–771. <https://doi.org/10.1080/02670844.2018.1551>
 46. Che H, Chu X, Vo P, Yue S (2018) Metallization of various polymers by cold spray. *J Therm Spray Technol* 27:169–178. <https://doi.org/10.1007/s11666-017-0663-1>

Publisher's note Springer Nature remains neutral with regard to jurisdictional claims in published maps and institutional affiliations.